Article

The Role of Strontium Enriched Hydroxyapatite and Tricalcium Phosphate Biomaterials in Osteoporotic Bone Regeneration

Janis Zarins [1,2,*] **, Mara Pilmane** [2] **, Elga Sidhoma** [2] **, Ilze Salma** [3] **and Janis Locs** [4]

[1] Department of Hand and Plastic Surgery, Microsurgery Centre of Latvia, Brivibas Street 410,
LV-1024 Riga, Latvia

[2] Institute of Anatomy and Anthropology, Riga Stradins University, Kronvalda boulevard 9, LV-1010 Riga,
Latvia; pilmane@latnet.lv (M.P.); Elga.Sidhoma@rsu.lv (E.S.)

[3] Department of Oral and Maxillofacial Surgery, Riga Stradins University, Dzirciema Street 20, LV-1007 Riga,
Latvia; salma.ilze@gmail.com

[4] Rudolfs Cimdins Riga Biomaterials Innovations and Development Centre of Riga Technical University,
Pulka Street 3, LV-1007 Riga, Latvia; janis.locs@rtu.lv

* Correspondence: janis.zarins@mcl.lv

check for
updates

Abstract: Background: Strontium (Sr) enriched biomaterials have been used to improve bone regeneration in vivo. However, most studies provide only two experimental groups. The aim of our study was to compare eleven different bone sample groups from osteoporotic and healthy rabbits' femoral neck, as it is the most frequent osteoporotic fracture in humans. Methods: Osteoporotic bone defects were filled with hydroxyapatite 30% (HA) and tricalcium phosphate 70% (TCP), 5% Sr-enriched HA_{30}/TCP_{70}, HA_{70}/TCP_{30}, or $Sr-HA_{70}/TCP_{30}$ granules and were compared with intact leg, sham surgery and healthy non-operated bone. Expression of osteoprotegerin (OPG), nuclear factor kappa beta 105 (NFkB-105), osteocalcin (OC), bone morphogenetic protein 2/4 (BMP-2/4), collagen I (Col-1α), matrix metalloproteinase 2 (MMP-2), tissue inhibitor of matrix metalloproteinase 2 (TIMP-2), interleukin 1 (IL-1) and interleukin 10 (IL-10) was analyzed by histomorphometry and immunohistochemistry. Results: Our study showed that $Sr-HA_{70}/TCP_{30}$ induced higher expression of all above-mentioned factors compared to intact leg and even higher expression of OC, MMP-2 and NFkB-105 compared to $Sr-HA_{30}/TCP_{70}$. HA_{70}/TCP_{30} induced higher level of NFkB-105 and IL-1 compared to HA_{30}/TCP_{70}. Conclusion: Sr-enriched biomaterials improved bone regeneration at molecular level in severe osteoporosis and induced activity of the factors was higher than after pure ceramic, sham or even healthy rabbits.

Keywords: strontium; rabbit, osteoporosis; femoral neck; calcium phosphate

1. Introduction

Osteoporosis is defined as a generalized skeletal disease with micro architectural bone changes and low mineral density, which leads to fragility and risk of fractures [1]. In the field of orthopedics, an osteoporotic femoral neck fracture is one of the most common and devastating injuries and, despite correct surgical fixation, avascular necrosis or metal implant dislocations can occur in up to 22.5% of bone surgery cases [2]. To overcome those complications, many attempts have been made to improve bone healing and mechanical stability of the prosthesis by creating physiologically active implant induced bone remodeling [3]. Bone tissue engineering (BTE) is a promising approach for treating bone defects by providing a template to guide bone regeneration [4]. Local support and stimulation of bone healing with good experimental and clinical results have been published before. For example, Herford

et al. found that addition of recombinant human bone morphogenetic protein type 2 to a collagen matrix, which is applied during distraction osteogeneis, increases faster bone tissue regeneration [5]. Poli et al. also reported that guided BTE, using titanium micromesh filled with bone grafts, provides sufficient bone volume correction in humans with severe alveolar atrophies [6]. Furthermore, clinical study by Chen et al. found an increase of bone healing and good bone to implant incorporation when biphasic calcium phosphate ceramics were used as a local treatment for comminuted fractures and fracture nonunion [7].

Bone tissue exist in a continual state of dynamic balance during the replacement of an old bone with a new one via a bone remodeling process [8]. One of the most popular recently studied metal is strontium (Sr), which has shown a unique activity in bone cells [9]. Sr can simultaneously affect antagonistic processes by increasing osteoblastogenesis and new bone formation, while decreasing osteoclastogenesis and bone resorption [10]. Animal studies have shown encouraging results when using biomaterials enriched with metallic ions providing local treatment of osteoporosis [11]. Rabbits have shown advantages over other species studied due to the faster bone turnover and active Haversian channel system, which is similar to humans' bone and crucial for evaluation of regenerative processes of the bone [12].

It is important to understand precise interactions between different morphogens, growth factors, cell activity indicators and immunity cytokines. In our study, we investigated the following markers: OPG, OC, NFkB-105, Col-1α, BMP-2/4, MMP-2, TIMP-2, IL-1, and IL-10. Osteoprotegerin (OPG) is a very important regulatory factor in the bone remodeling and it is secreted by osteoblasts inhibiting RANKL (receptor activator of nuclear factor kappa beta ligand) induced osteoclastogenesis [8]. Osteocalcin (OC) is a major non-collagenous protein with high affinity for calcium ions, which promotes absorption to hydroxyapatite in bone matrix, thus regulating bone mineralization process [13]. Nuclear factor kappa beta 105 (NFkB-105) is a member of the transcriptional factor family and is involved in many signaling pathways essential for normal cellular functions and RANKL induced osteoclastogenesis [14]. Moreover, others have reported that NFkB is responsible for production and mediation of such cytokines as TNF-α and IL-1 [15]. Collagen type Iα (Col-1α) is the most abundant protein in the extracellular matrix (ECM) of the bone [16] and during bone formation its molecules arrange into fibrils, which undergo mineralization via apatite crystal formation [17]. Bone morphogenetic proteins 2/4 (BMP-2/4) belong to the transforming growth factor family and play important roles during bone tissue development and regeneration, and, due to the osteoinductivity, can enhance new bone formation via activation of cell proliferation and differentiation [18]. Matrix metalloproteinases (MMP) belong to the major proteinase enzyme family responsible for degradation and turnover of the ECM in normal physiological conditions and in skeletal pathologies such as osteoporosis and rheumatoid arthritis [19]. MMP-2 or gelatinase A can cleave collagen, aggrecans, gelatins, fibronectin, laminin, tenascin-C, elastin and its up-regulation is found inside the fracture callus, mediating bone regeneration during fracture healing [20]. Tissue inhibitor of matrix metalloproteinase 2 (TIMP-2) belongs to the multifunctional protein family, which inhibits the catalytic activity of MMP-2 in the ECM space [21]. Highest activity of the TIMP-2 is found during bone matrix mineralization in mature osteoblasts, where it directly stimulates bone resorbing activity of osteoclasts [20]. A variety of cellular and tissue functions are regulated by interleukin 1 (IL-1), which is a pro-inflammatory cytokine that participates in the development, activity and survival of the osteoclasts and activates bone destruction in osteoporosis [22]. Contrarily, interleukin 10 (IL-10), as an anti-inflammatory cytokine, can inhibit bone resorption and reduce inflammatory reactions via downregulation of the pro-inflammatory cytokine synthesis [23].

When investigating new biomaterials in the field of regenerative medicine for the improvement of bone healing, it is necessarily to establish systemic bone conditions in vitro that are similar to those found in humans. None of the previously published studies on Sr-enriched biomaterial implantation provide more than two experimental groups and there is a lack of severe osteoporotic condition animal group in most of the studies. Therefore, we focused on simulating an analogous level of constant and

severe osteoporosis similar to postmenopausal bone disease. The femoral neck area was chosen as a bone defect area, as it is the most common osteoporotic fracture site. The aim of our study was to analyze previously described marker activity in eleven different bone conditions from osteoporotic and healthy rabbits' femoral neck to investigate the potential use of 5% Sr-enriched hydroxyapatite (HA, mass ratio: 30% and 70%) and tricalcium phosphate (TCP, mass ratio: 70% and 30%) biphasic ceramic applications for the local treatment of osteoporosis. Bone samples were also obtained from rabbits' femoral neck area of healthy, sham surgery-affected and intact leg of all operated animals. We found that $Sr-HA_{70}/TCP_{30}$ biomaterials induce most noticeable local changes of bone regeneration, improving expression of all analyzed markers. All changes were found in molecular level, while new bone formation stayed similar for 12 weeks in severe osteoporosis.

2. Results

During the experiment, two rabbits died. Both died after the second stage of the study—one after $Sr-HA_{70}/TCP_{30}$ implantation and the other after the sham surgery. Pathological examination of visceral organs did not show any correlation between the implantation and the cause of death. No other rabbits showed any sign of suffering from pain or any other pathological conditions.

2.1. Trabecular Bone Area

All operated rabbits showed significantly reduced trabecular bone area (TBA) compared to the healthy rabbits' bone (Figure 1). However, no statistical difference of TBA was found between operated and non-operated legs of all operated animals (Table 1). Similarly, in the group of $Sr-HA_{30}/TCP_{70}$, TBA was decreased by 40.4% compared to the healthy rabbits. TBA of pure HA_{30}/TCP_{70} was decreased by 42.5%, in $Sr-HA_{70}/TCP_{30}$ by 47.6% and pure HA_{70}/TCP_{30} by 43.3%. In the sham group, TBA was decreased by 38.4% compared to the healthy rabbits' bone.
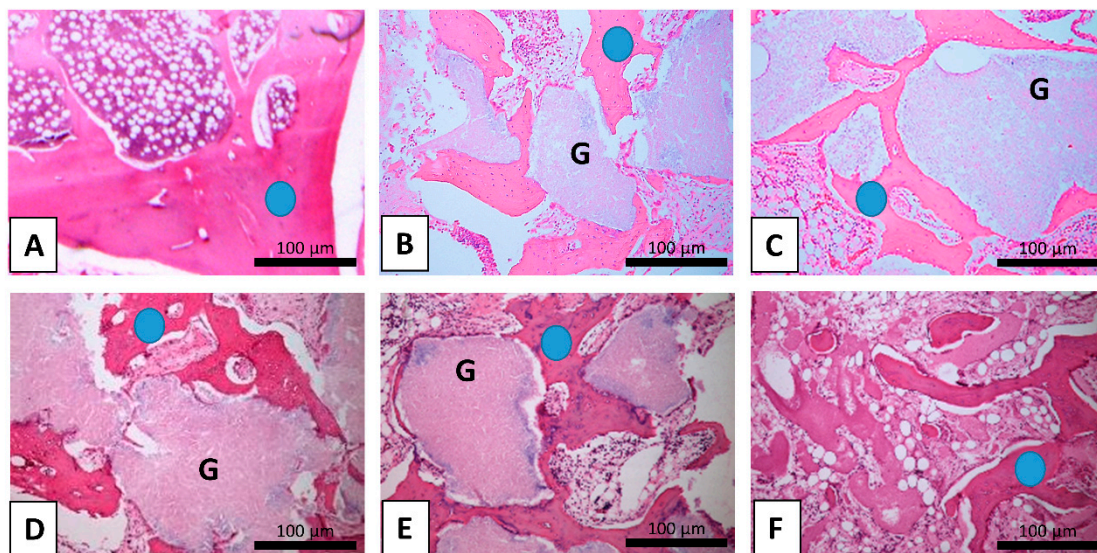

Figure 1. Trabecular bone area between study groups: (**A**) healthy rabbits' bone with nearly double TBA compared to: (**B**) ($Sr-HA_{30}/TCP_{70}$); (**C**) (HA_{30}/TCP_{70}); (**D**) ($Sr-HA_{70}/TCP_{30}$); (**E**) (HA_{70}/TCP_{30}); and (**F**) (sham). G, granules; blue dot, bone trabeculae; H&E staining; magnification $\times$ 100; scale bar, 100 µm.

Table 1. Summary of trabecular bone area and semi-quantitative analysis.

Variables Group	TBA, mm^2	OPG	OC	NFkB-105	BMP-2/4	Col-1α	MMP-2	TIMP-2	IL-1	IL-10
A										
Sr-HA$_{30}$/TCP$_{70}$	0.234	**3**^{c} (2.5–3)	**3**^{c} (2–3)	**2**^{c} (1.5–2)	**2.5**^{c} (1.5–3)	**3**^{c} (2–3)	**2** (1–3)	**3** (2.5–3)	**1**^{c} (0.5–1.5)	**2** (1.5–2.5)
Intact leg	0.226	**2** (2–2.5)	**2** (2–2.5)	**1** (1–1.5)	**1.5** (1–2)	**2** (2–3)	**1** (1–2)	**3** (2–3)	**0.5** (0–1)	**1.5** (1–2)
HA$_{30}$/TCP$_{70}$	0.226	**2**^{a} (2–3)^b	**2.5** (2–3)	**1.5**^{c} (1–2)	**2** (1–2)	**3** (2–3)	**2**^{c} (1.5–3)	**3** (2–3)	**1** (0–1.5)	**2** (2–2.5)
Intact leg	0.198	**2** (1.5–2.5)	**2** (1.5–3)	**1** (0–1.5)	**2** (1–2)	**2.5** (2–3)	**1.5** (1–1.5)	**2.5** (2–3)	**0.5** (0–1)	**2** (1.5–2.5)
B										
Sr-HA$_{70}$/TCP$_{30}$	0.206	**3**^{c} (2.5–3)	**3.5**^{c} (2.5–4)	**3**^{c} (2–3.5)	**2.5**^{c} (2–3)	**3**^{c} (2–3.5)	**2.5**^{c} (2–3)	**3**^{c} (2.5–3)	**1.5**^{c} (1–2)	**2.5**^{c} (2–3)
Intact leg	0.222	**2** (1.5–2)	**1.5** (1–3)	**2** (1.5–2)	**0.5** (0.5–1)	**1.5** (1–3)	**1.5** (1–2)	**2** (1.5–2.5)	**0.5** (0.5–1)	**1.5** (1–2)
HA$_{70}$/TCP$_{30}$	0.223	**2**^{c} (2–3)	**3**^{c} (2–4)	**2**^{c} (2–3)	**2**^{c} (1.5–2.5)	**2.5**^{c} (2.5–3)	**2.5**^{c} (2.5–3.5)	**3**^{c} (2.5–3.5)	**2**^{c} (1.5–2.5)	**2.5**^{c} (2–3)
Intact leg	0.212	**1.5** (1.5–2)	**2** (1–2)	**1.5** (1–2)	**0.5** (0.5–1.5)	**2** (1–2.5)	**1.5** (1–2)	**2** (1.5–2)	**0.5** (0.5–1)	**2** (1.5–2.5)
C										
Sham	0.242	**2** (2–2.5)	**2.5** (2–3)	**1.5** (1–2)	**2** (1.5–2)	**3**^{c} (2–3)	**2** (1–3)	**3** (2–3)	**1** (0.5–2)	**2.5** (2–3)
Intact leg	0.207	**2** (2–2.5)	**2** (2–2.5)	**1.5** (1–3)	**1.5** (1–2)	**2** (1.5–3)	**1.5** (1–3)	**3** (2–3)	**1** (0.5–2)	**2** (1–3)
D										
Healthy	0.393	**2.5** (2–3)	**3** (2.5–3)	**2** (1.5–2)	**1.5** (1–2)	**1.5** (1–2)	**2** (1–3)	**2.5** (2–2.5)	**0.5** (0–1)	**2** (1–2.5)

^{a} Numbers in bold are the adjusted mean values of semi-quantitative method; ^{b} Minimum and maximum value of immunopositive bone cells; ^{c} Statistically significant difference between operated leg and intact leg of analyzed factors.

2.2. Immunohistochemical Analysis

The study found a variability of analyzed factors among study groups. An overview of the obtained results is shown in the Table 1 and the appearance of positive bone cells is shown in Figure 2. Partial results and comparison within Groups A and B have been separately published before [24,25]. Only statistically significant results are reflected in the further paragraphs.

2.2.1. Group A

A higher appearance of OPG, OC, NFkB-105, BMP 2/4, IL-1 and Col-1α immunopositive osteocytes was found in bone samples after Sr-HA$_{30}$/TCP$_{70}$ granule implantation compared to intact leg ($p = 0.007$, U = 5.000; $p = 0.005$, U = 4.500; $p = 0.001$, U = 0.500; $p = 0.021$, U = 7.000; $p = 0.022$, U = 7.500; $p = 0.015$, U = 7.500).

Only a few factors were found to be higher after implantation of HA$_{30}$/TCP$_{70}$ granules compared to intact leg—NFkB-105 and MMP-2 ($p = 0.03$, U = 9.000; $p = 0.002$, U = 1.500).

Presence of Sr induced higher expression of OPG and NFkB 105 rather than pure HA$_{30}$/TCP$_{70}$ ($p = 0.04$, U = 9.500; $p = 0.01$, U = 6.000).

2.2.2. Group B

Sr-HA$_{70}$/TCP$_{30}$ induced a higher appearance of positive osteocytes of all factors compared to the intact leg: OPG, OC, NFkB-105, BMP 2/4, MMP-2, TIMP-2, IL-1, IL-10 and Col-1α ($p = 0.02$, U = 0.500; $p = 0.06$, U = 1.000; $p = 0.012$, U = 3.000; $p = 0.003$, U = 0.500; $p = 0.004$, U = 0.500; $p = 0.005$, U = 1.500; $p = 0.024$, U = 4.500; $p = 0.005$, U = 1.000; $p = 0.02$, U = 4.000).

Pure HA$_{70}$/TCP$_{30}$ showed similar outcome and higher appearance of immunopositive bone cells of all factors were found: OPG, OC, NFkB-105, BMP 2/4, MMP-2, TIMP-2, IL-1, IL-10 and Col-1α ($p = 0.029$, U = 15.000; $p = 0.001$, U = 2.500; $p = 0.011$, U = 10.000; $p = 0.001$, U = 1.000; $p = 0.004$, U = 6.000; $p = 0.001$, U = 1.500; $p = 0.001$, U = 0.500; $p = 0.016$, U = 10.000; $p = 0.003$, U = 5.000).

Sr-HA$_{70}$/TCP$_{30}$ induced higher expression of OPG rather than pure HA$_{70}$/TCP$_{30}$ ($p = 0.025$, U = 8.000).

2.2.3. Group C

Numerous Col-1α positive osteocytes were found after sham surgery, while only moderate number of them were found in non-operated leg ($p = 0.044$, U = 6.000).
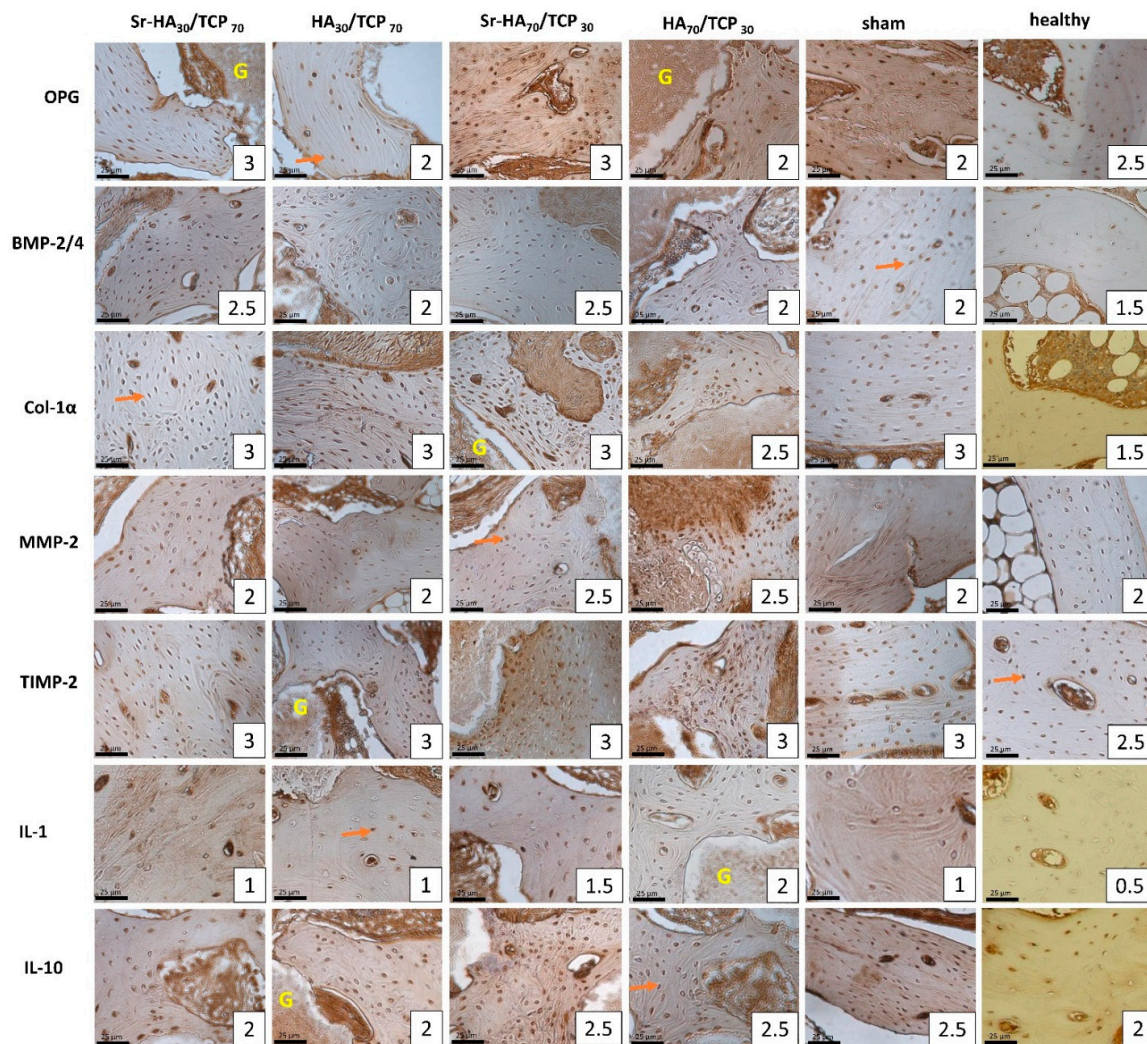
Figure 2. Distribution overview of the immunohistochemically analyzed factors. G, granules; red arrow, immunopositive bone cells. Numbers in lower right sided text box are quantified according to semi-quantitative method and are graded as follows: 0, no positive bone cells; 0.5, no to few positive bone cells; 1, few positive bone cells; 1.5, few to moderate bone cells; 2, moderate number of immunopositive bone cells; 2.5, moderate to numerous bone cells; 3, numerous immunopositive bone cells. IMH, magnification $\times$ 100, scale bar 25 μm.

2.2.4. Healthy Bone Compared to Operated Bone Samples

Group A

Both biomaterial subgroups with or without strontium showed similar results and expression of the following factors were higher than in healthy bone samples: BMP 2/4, TIMP-2, IL-1 and Col-1α ($p = 0.004$, U = 6.500; $p = 0.031$, U = 14.500; $p = 0.002$, U = 6.000; $p = 0.004$, U = 7.000; $p = 0.016$, U = 12.000; $p = 0.032$, U = 0.500 $p = 0.001$, U = 0.500; $p = 0.001$, U = 0.500).

Number of OPG and NFkB105 positive bone cells were higher in healthy bone compared to HA_{30}/TCP_{70} bone samples ($p = 0.033$, U = 14.500; $p = 0.007$, U = 9.500).

Group B

Slight difference between $Sr-HA_{70}/TCP_{30}$ and HA_{70}/TCP_{30} bone samples were detected when compared to healthy bone. Only OPG positive bone cells were higher in healthy bone compared to pure biomaterial ($p = 0.049$, U = 19.500).

HA$_{70}$/TCP$_{30}$ induced higher expression of immunopositive bone cells of BMP 2/4, TIMP-2, IL-1, IL-10, and Col-1α compared to healthy bone (p = 0.009, U = 12.000; p = 0.003, U = 9.000; p = 0.0001, U = 0.500; p = 0.025, U = 16.000; p = 0.0001, U = 0.500).

Sr-HA$_{70}$/TCP$_{30}$ showed higher amount of OC, NFkB-105, BMP 2/4, TIMP-2, IL-1 and Col-1α immunopositive osteocytes compared to healthy bone (p = 0.023, U = 10.500; p = 0.016, U = 10.000; p = 0.002, U = 3.000; p = 0.002, U = 3.000; p = 0.002, U = 3.000; p = 0.001, U = 0.500)

Group C

Sham bone showed higher expression of TIMP-2, IL-1 and Col-1α compared to healthy bone (p = 0.010, U = 7.00; p = 0.023, U = 10.500; p = 0.001, U = 0.500), while OPG and OC immunopositive osteocytes were higher in healthy group (p = 0.018, U = 10.000; p = 0.047, U = 15.000).

2.2.5. Comparison Between Operated Groups

Group A and Group B

After the implantation of Sr-HA$_{70}$/TCP$_{30}$ ceramics OC, NFkB-105 and MMP-2 immunopositive bone cells were significantly higher compared to Sr-HA$_{30}$/TCP$_{70}$ granule implantation (p = 0.022, U = 5.500; p = 0.014, U = 6.00; p = 0.033, U = 6.500).

Similarly, only a few factors showed difference between pure biomaterial implantation, where HA$_{70}$/TCP$_{30}$ showed higher appearance of NFkB-105 and IL-1 immunopositive osteocytes compared to HA$_{30}$/TCP$_{70}$ (p = 0.002, U = 2.500; p = 0.037, U = 11.00).

Group A and Group C

Only OPG immunopositive osteocytes were higher after Sr-HA$_{30}$/TCP$_{70}$ biomaterial implantation compared to sham surgery (p = 0.023, U = 6.000).

Group B and Group C

Similarly, Sr-HA$_{70}$/TCP$_{30}$ biomaterials induced higher expression of OPG and OC compared to sham surgery without implantation (p = 0.027, U = 1.000; p = 0.034, U = 1.000).

Numerous NFkB-105 positive osteocytes were found after sham surgery compared to moderate to numerous after pure HA$_{70}$/TCP$_{30}$ (p = 0.042, U = 3.000).

2.2.6. Comparison Between Intact Leg Bone Samples of the Operated Groups

In Groups A and B, no statistical difference was obtained between intact leg bone samples.

Sham bone samples showed higher expression of NFkB-105 and TIMP-2 compared to Sr-HA$_{30}$/TCP$_{70}$ (p = 0.04, U = 8.500; p = 0.015, U = 3.500).

Sr-HA$_{70}$/TCP$_{30}$ showed higher expression of NFkB-105 and TIMP-2 compared to Sr-HA$_{30}$/TCP$_{70}$ (p = 0.003, U = 1.500; p = 0.049, U = 8.000), while Sr-HA$_{30}$/TCP$_{70}$ showed higher appearance of immunopositive BMP 2/4 osteocytes (p = 0.01, U = 4.000).

2.3. Correlation Between the Analyzed Factors

Statistically significant correlations are shown in Table 2. Strong and very strong either positive or negative correlations were considered relevant. All analyzed bone samples, except Sr-HA$_{70}$/TCP$_{30}$ showed interrelation correlations.

Table 2. Spearman rank correlation within groups.

Group	Variables	Correlation	Coefficient	*p* value
	A			
Sr-HA$_{30}$/TCP$_{70}$	NFkB-105 and Col-1α	SP	$r_s = 0.734$	$p = 0.046$
	TBA and Col-1α	VSP	$r_s = 0.809$	$p = 0.028$
	OC and NFkB-105	VSP	$r_s = 0.833$	$p = 0.020$
	OC and IL-1	SP	$r_s = 0.772$	$p = 0.042$
	NFkB-105 and Il-1	VSP	$r_s = 0.814$	$p = 0.026$
HA$_{30}$/TCP$_{70}$	MMP-2 and TIMP-2	SN	$r_s = -0.764$	$p = 0.046$
	Col-1α and Il-1	VSP	$r_s = 0.814$	$p = 0.026$
	NFkB-105 and Col-1α	SP	$r_s = 0.767$	$p = 0.044$
	OC and TBA	VSN	$r_s = -0.837$	$p = 0.019$
	B			
Sr-HA$_{70}$/TCP$_{30}$	-	-	-	-
	OC and MMP-2	SP	$r_s = 0.736$	$p = 0.037$
HA$_{70}$/TCP$_{30}$	OPG and IL-10	VSN	$r_s = -0.816$	$p = 0.013$
	OC and Col-1α	SN	$r_s = -0.732$	$p = 0.039$
	C			
	NFkB-105 and MMP-2	VSP	$r_s = 0.939$	$p = 0.005$
Sham	NFkB-105 and IL-1	VSP	$r_s = 0.833$	$p = 0.039$
	OPG and IL-10	VSN	$r_s = -0.880$	$p = 0.021$
	D			
	BMP 2/4 and Col-1α	VSP	$r_s = 0.829$	$p = 0.003$
	OC and BMP 2/4	SP	$r_s = 0.634$	$p = 0.049$
	MMP-2 and IL-10	SP	$r_s = 0.650$	$p = 0.042$
Healthy	TBA and NFkB-105	SP	$r_s = 0.657$	$p = 0.039$
	NFkB-105 and MMP-2	SN	$r_s = -0.670$	$p = 0.034$
	NFkB-105 and Col-1α	SN	$r_s = -0.646$	$p = 0.044$
	TBA and TIMP-2	SN	$r_s = -0.690$	$p = 0.027$
	TBA and IL-1	SN	$r_s = -0.783$	$p = 0.007$

TBA, trabecular bone area; SP, strong positive; VSP, very strong positive; SN, strong negative; VSN, very strong negative.

3. Discussion

Preclinical evaluation of the safety and effectiveness of new experimental biomaterials for the local treatment of osteoporosis requires investigation of dynamic trabecular and cortical bone remodeling [26]. Moreover, the evaluation of the mechanical properties and biocompatibility of the biomaterial is a crucial step for choosing a suitable animal model [27].

Almost every animal model has its own advantages and disadvantages, therefore relevant aspects about bone type, remodeling, life span, adaptability to experimental manipulation and economic factors should be considered. Smaller animals, such as rats or mice, are suitable for housing, but have a short lifespan and their bone homeostasis is completely different form human bone [28]. Wancket et al. evaluated most commonly used animal models and found that dogs are preferably used in dental studies due to the spontaneous periodontitis, but the main disadvantages are that the bone remodeling and apposition can vary within and between the dogs. In pigs' bone anatomy, remodeling rate and bone mineral density are similar to human bone, but the limitations are pigs' excessive body weight, difficult handling of the animal and relatively short extremities, which could affect the evaluation of orthopedic implants. Sheep and goat experimental models have increased during the last years due to relatively vertical alignment of the cervical vertebrae, which provides similar axial compression and rotation forces to the human spine. However, the main drawbacks are that sheep cortical bone remains predominant at 7–9 years of age, it undergoes seasonal bone loss and sheep and goats have more dense and stronger bones when compared to humans bone [29].

Rabbits lately have been the most widely used experimental animals for the evaluation of bone regenerative properties after different biomaterial implantation [30]. This is because the maturity of rabbits is achieved at 7–8 months, which is faster than for other medium-sized animals [31]. Rabbits' bone shows quite rapid bone resorption and formation, and intracortical remodeling with active Haversian channel system is similar to humans' bone. Moreover, rabbits are easy to handle, while induction of osteoporosis is relatively short and technically uncomplicated [26]. Others have reported that fracture toughness and bone mineral density are proportionally similar to humans' physiological and pathological conditions [32]. Human osteoporosis is defined as reduction of bone mineral density of more than 25%. Baofeng et al. conducted a study to establish a consistent osteoporosis model, where combination of ovarectomy and corticosteroid treatment in a dose of 1 mg/kg/day was used. Such dose of methylprednisolone was used because it has no side effects to other bone structures, for example, higher dose could induce cartilage damage. They found that ovarectomy and systemic injections of corticosteroids decrease bone mineral density by about 36% [26]. This protocol nowadays is used to induce constant osteoporosis, similar to our study. We found noticeable decrease in TBA between healthy rabbits and the experimental ones: the mean TBA in healthy rabbits was 0.393 mm^2, and in operated animals it was from 0.206 mm^2 to 0.242 mm^2, which is a 38–48% decrease. Our findings suggest that the established level of osteoporosis inducing bone remodeling changes was severe. If real orthopedic implants are investigated, the disadvantage of using rabbits could be the small size of the rabbits' bone [27]. In our study, we chose to establish a non-critical bone defect in rabbits femoral neck area, as it is an increasing problem for humans, being the most affected osteoporotic fracture. Other authors have used mandible, tibial or distal femur critical or non-critical bone defects for biomaterial applications [33,34].

Our study included four main groups: two biphasic calcium phosphate ceramics with different mass ratio of HA_{30}/TCP_{70} and HA_{70}/TCP_{30}, a sham group with constant osteoporotic conditions, and healthy intact bone controls. The first two groups were further divided into Sr-enriched and pure ceramic bone. Bone samples from contralateral intact leg in osteoporotic animals were also evaluated, thus local peri-implant and generalized condition changes were analyzed. In total, 11 different bone sample groups were analyzed. None of the previously published studies on Sr-enriched biomaterials provide analysis of so many sample groups using the same methodology.

In a systematic review, Neves et al. presented a summary of Sr-enriched biomaterial applications for bone regeneration. They included 27 in vivo original studies where at least two groups with identical biomaterials with and without Sr were evaluated. The authors concluded that Sr-enriched biomaterials are safe and effective for the stimulation of bone remodeling. However, analyzed studies differ one from other by animal model, biomaterial, analyzed measurements and study methods. Only 9 out of 27 were done on rabbits and none used osteoporotic animal model (Table 3) [10]. This makes further comparison with other studies difficult due to the lack of osteoporotic condition of the experimental group.

Table 3. Profile of studies using Sr-enriched biomaterials in rabbits.

Author	Status	Number		Defect, mm	Localization	Material	Time, Weeks	New Bone	Bone Remodeling
		E	C						
Dagang [35]	H	2	2	2.2	distal femur	Sr-HA	24	similar	increased
Gu [36]	H	12	12	15	radius	Sr-CPP	16	increased	increased
Mohan [37]	H	6	6	15	ulna	Sr-CP	12	increased	increased
Tian [38]	H	24	24	15	radius	Sr-CPP	16	increased	similar
Kang [39]	ON	18	18	3	proximal femur	Sr-CPP and MNC	12	increased	increased
Tarafder [40]	H	2	2	5.5	distal femur	B-TCP-MgO/SrO	12	increased	increased
Xie [41]	H	9	9	15	femoral shaft	K/Sr-CPP	12	increased	increased
Zhang [42]	H	6	6	6	distal femur	Sr-BBG	8	increased	increased

H, healthy; ON, osteonecrosis; E, experimental; C, control; Sr, strontium; HA, hydroxyapatite; CPP, calcium polyphosphate; CP, calcium phosphate; MNC, mononuclear cells; TCP, tricalcium phosphate; Mg, magnesium; BBG, bioactive borate glass.

Implanted biomaterials interact in chemical, physical and biological ways with the recipient biological system [43]. Calcium phosphate ceramics (CPC) are similar to natural bone, thereby providing excellent osteoconductivity, which allows migration, proliferation and differentiation of the osteoprogenitor cells and deposition of ECM. HA and TCP possess strong osteoinduction: it allows facilitation of nutrition and oxygen between bone tissue and biomaterial and stimulates the differentiation of the stem cells due to the released calcium and phosphate ions, which form environment for cell migration. CPC can form a direct bond between implant and host bone [44]. HA has low solubility and is biocompatible with the bone homeostasis, while TCP improves osteoconduction due to the rapid degradation [7]. Biodegradation of the implanted biomaterial occurs simultaneously along with bone formation and remodeling. Calcium phosphate materials undergo biodegradation via dissolution, but the speed of the dissolution depends on crystallinity and porosity [45]. Moreover, Wang et al., in a literature review of biomaterials, pointed out that relatively high Ca/P ratio and crystallinity delay the resorption rate of HA, which is regulated by giant cell and macrophage mediated processes [11]. Implanted biomaterials trigger a foreign body reaction, a cascade of complex response of exposed tissue, starting with vascular damage and absorption of plasma proteins onto the foreign body surface, which initiates activation of macrophage fusion to form multinucleated giant cells and generation of functional vessels and surround the object by fibrotic capsule [46]. Biocompatible materials undergo early resolution of acute and chronic inflammatory responses, usually lasting no longer than two weeks, following by granulation tissue and fibrotic capsule formation at the biomaterial interface [47]. Biphasic calcium phosphate ceramics increase high number of giant cells, which is comparable to pure TCP within 15 days after implantation, while reduction of giant cell formation after 15 days is comparable to properties of pure HA [48]. Tachibana et al. found no intermediate layer of fibrotic tissue between ceramic interface and direct contact of the bone, while granules with partial contact with existing bone were surrounded by fibrotic tissue [49]. Similarly, we did not find any specific foreign body reaction around implanted granules with close contact to bone 12 weeks after implantation. Therefore, biphasic calcium phosphate overcomes those disadvantages when HA and TCP have been used alone [11].

Strontium can incorporate into ion exchange during bone remodeling via similarity in the size and behavior to calcium ions, which allows Sr to affect some osteoblast mediated processes by activating calcium sensing receptors (CaSR) in osteoblasts and stimulating the expression of local growth factors [3]. Increase of Sr ions around the CPC reduces crystallinity and alters the crystal lattices, improving solubility of biomaterial [50]. Sr can induce other signaling pathways through CaSR: activation of ERK1/2 (extracellular signal related kinase) increases the rate of osteoblast replication and activation of Akt (protein kinase) mediates anti-apoptotic effect on osteoblasts. Osteogenesis is also improved via Wnt (wingless-related integration site) signaling pathway, where Sr decreases expression of sclerostin, which is an inhibitor of Wnt. Likewise, osteoblast replication is improved via activation of NFATc1 (nuclear factor of activated T cells), which is important transcription factor regulating gene expression in bone remodeling [11]. However, there is no strong evidence based on human data to confirm the implanted biomaterial biodegradability and involved complex signaling cascades using enriched bioresorbable materials [51].

Most studies presented in Table 3 show increased bone formation in the experimental groups, however none of them represent constant osteoporosis similar to our study. We found almost equal TBA among all experimental groups, as well as similar bone area between operated and non-operated leg bone samples 12 weeks after surgery. No difference was found also among HA and TCP ratio (30/70 or 70/30). Baier et al., albeit in osteoporotic rats, found no difference in new bone formation after 12 weeks, but only after 24 weeks Sr-enriched calcium phosphate cement showed increase of new bone [50]. These findings suggest that the severity of osteoporosis affects biodegradation and solubility of HA and TCP, as well as dissolution of Sr ions to increase new bone formation. Thus, prolonged observation time is needed for proper assessment of new bone formation. In our study, healthy bone samples showed strong correlation between TBA and higher expression of NFkB-105, which intends

high cell activity within normal homeostatic bone remodeling conditions, as well as lower expression of Il-1, which clearly indicates its role as inducer of bone resorption. Contrarily, in $Sr-HA_{30}/TCP_{70}$ bone samples, strong correlations were found among TBA, Col-1α, and Il-1, suggesting its other mechanisms of participating in new bone formation processes in severe osteoporotic bone conditions.

The immunohistochemical analysis revealed significant changes of analyzed markers between bone conditions in our study. Induction of local bone tissue response was observed while comparing intact bone samples versus operated bone samples. Our findings revealed that presence of the Sr after implantation of $Sr-HA_{30}/TCP_{70}$ granules showed noticeable increase of OPG, OC, NFkB-105, BMP 2/4, IL-1, Col-1α and additionally MMP-2, TIMP-2 and IL-10 expressions were higher after $Sr-HA_{70}/TCP_{30}$ compared to contralateral femur bone. Much smaller difference was found after the implantation of pure HA/TCP within both mass ratios. Likewise, after sham surgery, only Col-1α was higher in the operated leg. This confirms previous findings of Jebahi et al., who detected no difference of Sr concentration in animal blood serum and excretion, suggesting only local role of Sr effects after implantation of Sr-enriched biomaterials [52]. Histomorphometric results reveal that systemic release of Sr from the ceramic implants did not lead to sufficiently high serum strontium levels to induce significant systemic effects on bone mass in the rat model [50]. In addition, similar expression of IL-1 was found in all experimental groups, even after sham surgery. The level of IL-1 was higher after surgery compared to healthy bone samples, while stable amount of IL-10 positive bone cells was found between operated and healthy bone samples.

In our osteoporotic rabbit model, we found an increase of OPG expression after implantation of both Sr-enriched HA/TCP granules, rather than when pure HA/TCP was used. The level of OPG was even higher than in healthy bone controls. It is important to emphasize the OPG role in the bone remodeling, because OPG decreases osteoclast formation and bone resorption activity, which are the dominant actions in osteoporosis [8]. Increase of osteoprotegerin expression was found by Thormann et al. in ovariectomized rats' femur after six weeks of Sr-CPP implantation in comparison to pure CPP and sham bone. They speculated that improved behavior of the degradation and better fragmentation of ceramics are related to the multinuclear cells and that the high levels of OPG do not impair biomaterial degradation due to the anti-osteoclastic effect [53]. In both Sr-enriched biomaterials, we did not find any significant correlation between OPG and other factors, suggesting its independent and important role in regulation of osteoclast mediated bone resorption even in severe osteoporosis.

Thormann et al. found significantly higher gene expression of alkaline phosphatase, Col-1 and OC in Sr-CPC, compared to pure CPC in ovariectomized rats' femur, while only noticeable increase of BMP-2 was found [53]. Similarly, our results reveal slight increase of BMP-2/4 and OC after Sr-enriched biomaterials compared to pure ceramics. Tarafder et al. found higher expression of OC in Sr doped TCP bone compared to sham surgery in healthy rabbits' femoral condyle defect [54]. Similarly, we too found higher expression of OC after $Sr-HA_{70}/TCP_{30}$ compared to sham, while other biomaterials showed similar distribution of immunopositive bone cells. Moreover, numerous to abundant OC positive osteocytes were found after $Sr-HA_{70}/TCP_{30}$ compared to numerous in $Sr-HA_{30}/TCP_{70}$ bone samples.

Xie et al. found that higher expression of MMP-2 was found after Sr-CPP scaffolds in healthy rabbits' femur, compared to pure CPP ceramics, suggesting higher ECM synthesis and more ECM repair of the bone defect [41]. In our study, moderate to numerous MMP-2 positive osteocytes were detected after $Sr-HA_{70}/TCP_{30}$ implantation, compared to moderate after $Sr-HA_{30}/TCP_{70}$. We can therefore speculate that a higher concentration of hydroxyapatite regulates slower dissolution of Sr ions, thus improving bone mineralization and higher rate of old ECM repair in severe osteoporosis. These findings are supplemented by results when pure HA/TCP were used: only NFkB-105 and Il-1 were higher after HA_{70}/TCP_{30} compared to HA_{30}/TCP_{70} induced bone regenerative cell activity.

Tian et al. found higher expression of Col-1 and BMP after Sr-enriched calcium polyphosphate implantation compared to pure CPP in healthy rabbits' bone [38]. Our results revealed similar distribution of Col-1α between all bone samples after biomaterial implantation. However, healthy rabbits showed almost two times lower Col-1α immunopositive bone cells compared to Sr-enriched

biomaterials. BMP 2/4 expression was similar within all operated animals, but higher compared to healthy ones. As BMP-2/4 indicates nearly new bone formation as osteoinductive factor, its equal distribution is associated with similar trabecular bone area within operated animals, suggesting that 12 weeks are insufficient to overcome suppressed bone regeneration in severe osteoporosis.

Our study possesses several limitations. Firstly, despite some common architectural and physiological properties between rabbits' and human bone, the difference is outstanding and obtained results are only with a predictable value. Secondly, further studies on bigger animals with osteoporotic femoral neck fracture fixation using Sr-enriched metal implants is needed to obtain more relevant information on bone regeneration. Thirdly, the use of semi-quantitative method for evaluating immunohistochemistry data could misinterpret the results as being partly subjective. To overcome this limitation further study results should be analyzed by polymerized chain reaction, Western blotting or ELISA. Fourthly, as we obtained similar new trabecular bone area between operated animals, prolonged experiment time is needed in such severe osteoporotic bone conditions for proper qualitative and quantitative assessment of the results.

4. Materials and Methods

4.1. Ethics Statement

The experimental animal project was approved with a permission of Animal Ethics Committee of Food and Veterinary Administration of Latvia (No. 72/2015).

4.2. Biomaterial Preparation

Bioceramic materials were prepared through an aqueous precipitation using calcium oxide (CaO, puriss., Fluka), strontium oxide obtained from strontium carbonate ($SrCO_3$, reagent-grade, Sigma-Aldrich) and 2M aqueous solution of orthophosphoric acid (H_3PO_4, puriss., 75%, Sigma-Aldrich). The method was adapted from previous works [55,56]. Aqueous solution of 2M H_3PO_4 was added to the starting suspensions of $Ca(OH)_2$ or $Sr(OH)_2/Ca(OH)_2$. (Ca+Sr)/P molar ratios were varied to obtain bioceramic materials with desired HAp/β-TCP phase ratios (30/70 or 70/30). Filtered precipitates were used for production of granules by extrusion through a 1.4 mm mesh with following drying at 80 °C for 20 h and sintering at 1150 °C for 2 h. After sintering the prepared granules were sieved and granule fraction between 0.5 and 1 mm were selected for experiments as potentially usable as a bone filler. Prior to application, the dried granules were sterilized using steam sterilization. The field emission scanning electron microscopy (FE-SEM) of the sintered ceramic granules is shown in Figure 3.
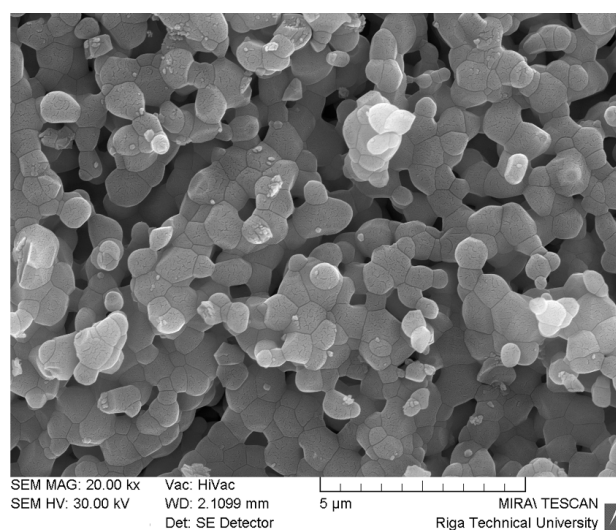

Figure 3. FE-SEM micrograph of sintered ceramic granules.

4.3. Design of the Experiment.

4.3.1. Animal Model

Forty-six California female matured rabbits (8 months old) were used for the experiment. Thirty-six of them underwent experimentally induced osteoporosis, while 10 formed control group of healthy animals. During the observational period all rabbits were kept in conformable fencings with unrestricted movements and nutrition ad libitum. Daily behavior habits, appearance and nutrition were evaluated.

4.3.2. Induction of Osteoporosis

In the first stage, simulation of postmenopausal osteoporosis was created by elimination of feminine gonads to decline estrogen hormone levels, which increase activation of bone remodeling in favor of bone resorption. Surgery was done under general anesthesia with 30 mg/kg ketamine, 3 mg/kg xylazine and 0.1–0.5 mg/kg atropine. Abdomen of rabbits was opened through a midline of linea alba and bilateral ovarectomy was done by ligation of both ovaries. The abdominal wall was closed without any tension. Postoperatively subcutaneous ketoprofen 1–3 mg/kg injections were used for pain management and stiches from skin were removed on the 10th day after surgery. Assessment of the rabbits was done on 14th day to convince properly healed wound without any signs of inflammation. During the following six weeks, intramuscular injections of methylprednisolone at a dose of 1 mg/kg were done every day to create severe osteoporosis with weak regenerative potential.

4.3.3. Biomaterial Implantation

After six-week continuous glucocorticoid administration, all rabbits underwent a second surgery. A 2 cm longitudinal incision was made in the right trochanter major area of the femur bone. Under controlled hemostasis, thigh muscles and periosteal tissue were divided until bone cortex. Trephine burr drill was used to create 5 mm wide non-critical bone defect (4 mm in depth) in the femoral neck area. All rabbits were divided into three groups: in Group A, bone defect was filled with HA/TCP (ratio 30/70), while, in Group B, with HA/TCP (ratio 70/30), and both groups with and without 5% Sr. In Group C, bone defect was left unfilled for secondary healing. Subgrouping of experimental animals are shown in Table 4. All surgical steps were performed by the same specialists for all groups.

Table 4. Distribution of rabbits between the groups.

Californian Female Rabbits					
Group	**A**		**B**		**C**	**D**
Status	Sr-HA/TCP	HA/TCP	Sr-HA/TCP	HA/TCP	sham	healthy
Ceramic ratio	30/70	30/70	70/30	70/30	-	-
Number	7	7	7	8	7	10

4.3.4. Harvest of Bone Samples

Twelve weeks after the implantation surgery, euthanasia was performed using general anesthesia by intrapulmonal T-61 administration. For further bone analysis, samples were taken from the operated leg for the assessment of local tissue quantitative and qualitative changes and from non-operated legs femoral neck area to evaluate systemic bone tissue changes. Bone samples from the same area were harvested from healthy rabbits.

4.4. Routine Morphology and Immunohistochemistry

All bone samples were preserved in Stefanini's solution directly after the harvest. The next stages were performed in the Laboratory of Morphology of the Institute of Anatomy and Anthropology, Riga, Latvia by certified specialists. Bone samples were decalcified, dehydrated, embedded in paraffin

and 3–5 μm tissue sections were made and prepared for hematoxylin and eosin (H&E) staining reactions [57]. Immunohistochemistry (IMH) was performed using biotin-streptavidin standard protocol [58]. Immunostaining was done using the following antibodies: OPG (obtained from rabbit, 1:100 dilution, Biorbyt, USA), OC (obtained from rabbit, 1:100 dilution, Biorbyt, USA), COL-1 (obtained from rabbit, 1:100 dilution, Biorbyt, USA), NFkB-105 (obtained from rabbit, 1:100 dilution, Abcam, UK), BMP-2/4 (obtained from goat, 1:100 dilution, R&D systems, UK), MMP-2 (obtained from rabbit, 1:100 dilution, Biorbyt, USA), TIMP-2 (obtained from mouse, 1:100 dilution, SANTA CRUZ BIOTECHNOLOGY, USA), IL-1 (obtained from rabbit, 1:100 dilution, Biorbyt, USA) and IL-10 (obtained from rabbit, 1:100 dilution, ABBIOTEC, LLC, USA).

A semi-quantitative method was used for the evaluation of the relative amount of immunostaining positive bone cells and was graded as follows: "0" (0), no positive structures; "+" (1), few positive structures; "++" (2), moderate number of positive structures; "+++" (3), numerous positive structures; and "++++" (4), abundance of positive structures seen in visual field [59]. Numbers in brackets were adjusted for the statistical analysis.

Trabecular bone area was calculated by randomly choosing three equal fields of view (0.975 mm^2) and measured using Image Pro plus 7 program.

4.5. Statistics

IBM SPSS v23 (USA) statistical program was used for statistical analysis using the Mann–Whitney U tests and Spearman's rank correlation coefficient. All evaluations were two-tailed and statistical significance was detected if value of $p < 0.05$.

5. Conclusions

Sr-enriched biomaterials induced most noticeable local activity of biomarkers relevant for bone remodeling even in severe constant osteoporotic bone. $Sr-HA_{70}/TCP_{30}$ showed superior impact on bone remodeling and regeneration compared to other biomaterials or sham. It increased expression of OPG, OC, NFkB-105, BMP-2/4, MMP-2, TIMP-2, Col-1α, Il-1 and Il-10 compared to intact leg bone and improved mineralization, extracellular matrix turnover and cellular activity in comparison to $Sr-HA_{30}/TCP_{70}$. Our findings suggest that implantation of biomaterials with or without strontium induced higher activity of bone regeneration than in healthy animals, excluding trauma role for induction of regeneration. The mass ratio of HA and TCP had an impact on release of Sr ions during biomaterial solubility in favor of HA_{70}/TCP_{30} mass ratio. After 12 weeks of implantation, in severe osteoporotic conditions, bone regenerative properties were induced at molecular level, while quantitative increase of new trabecular bone is not confirmed yet.

Author Contributions: Conceptualization: I.S. and J.L.; Methodology: M.P.; Software: J.Z.; Validation: J.Z., M.P. and E.S.; Formal Analysis: J.Z., M.P. and E.S.; Resources, M.P., I.S. and J.L.; Data Curation: J.Z.; Writing—Original Draft Preparation, J.Z.; Writing—Review and Editing, J.Z., M.P., and E.S.; Visualization, J.Z.; Supervision, M.P. and E.S.; and Funding Acquisition, M.P. and J.L.

Conflicts of Interest: The authors declare no conflict of interest.

References

1. Metcalfe, D. The pathophysiology of osteoporotic hip fracture. *Mcgill. J. Med.* **2008**, *11*, 51–57.
2. Xu, D.F.; Bi, F.G.; Ma, C.Y.; Wen, Z.F.; Cai, X.Z. A systematic review of undisplaced femoral neck fracture treatments for patients over 65 years of age, with a focus on union rates and avascular necrosis. *J. Ortho Surg. Res.* **2017**, *12*, 28. [CrossRef] [PubMed]
3. Offermanns, V.; Andersen, O.Z.; Riede, G.; Sillassen, M.; Jeppesen, C.S.; Almtoft, K.P.; Talasz, H.; Öhman-Mägi, C.; Lethaus, B.; Tolba, R.; et al. Effect of strontium surface-functionalized implants on

early and late osseointegration: A histological, spectrometric and tomographic evaluation. *Acta Biomater.* **2018**, *69*, 385–394. [CrossRef] [PubMed]

4. El-Rashidy, A.A.; Roether, J.A.; Harjaus, L.; Kneser, U.; Boccaccini, A.R. Regenerating bone with bioactive glass scaffolds: A review of in vivo studies in bone defect models. *Acta Biomater.* **2017**, *62*, 1–28. [CrossRef] [PubMed]

5. Herford, S.A.; Cicciu, M.; Eftimie, L.F.; Miller, M.; Signorino, F.; Fama, F.; Cervino, G.; Giudice, G.L.; Bramanti, E.; Lauritano, F.; et al. rhBMP-2 applied as support of distraction osteogenesis: A split-mouth histological study over nonhuman primates mandibles. *Int. J. Clin. Exp. Med.* **2016**, *9*, 17187–17194.

6. Poli, P.P.; Beretta, M.; Cicciù, M.; Maiorana, C. Alveolar ridge augmentation with titanium mesh. A retrospective clinical study. *Open Dent. J.* **2014**, *8*, 148–158. [CrossRef] [PubMed]

7. Chen, Y.J.; Pao, J.I.; Chen, C.S.; Chen, Y.C.; Chang, C.C.; Hung, F.M.; Chang, C.H. Evaluation of New Biphasic Calcium Phosphate Bone Substitute: Rabbit Femur Defect Model and Preliminary Clinical Results. *J. Med. Biol. Eng.* **2017**, *37*, 85–93. [CrossRef] [PubMed]

8. Tong, X.; Gu, J.; Song, R.; Wang, D.; Sun, Z.; Sui, C.; Zhang, C.; Liu, X.; Bian, J.; Liu, Z. Osteoprotegerin inhibit osteoclast differentiation and bone resorption by enhancing autophagy via AMPK/mTOR/p70S6K signaling pathway in vitro. *J. Cell. Biochem.* **2018**. [CrossRef] [PubMed]

9. Han, J.; Wan, P.; Ge, Y.; Fan, X.; Tan, L.; Li, J.; Yang, K. Tailoring the degradation and biological response of a magnesium-strontium alloy for potential bone substitute application. *Mater. Sci. Eng. C Mater. Biol. Appl.* **2016**, *58*, 799–811. [CrossRef] [PubMed]

10. Neves, N.; Linhares, D.; Costa, G.; Ribeiro, C.C.; Barbosa, M.A. In vivo and clinical application of strontium-enriched biomaterials for bone regeneration: A systematic review. *Bone Joint Res.* **2017**, *6*, 366–375. [CrossRef] [PubMed]

11. Wang, W.; Yeung, K. Bone grafts and biomaterials substitutes for bone defect repair: A review. *Bioactive Mater.* **2017**, *2*, 224–247. [CrossRef] [PubMed]

12. Wen, X.X.; Xu, C.; Wang, F.Q.; Feng, Y.F.; Zhao, X.; Yan, Y.B.; Lei, W. Temporal changes of microarchitectural and mechanical parameters of cancellous bone in the osteoporotic rabbit. *Biomed. Res. Int.* **2015**, *263434*. [CrossRef] [PubMed]

13. Rathore, B.; Singh, M.; Kumar, V.; Misra, A. Osteocalcin: An emerging biomarker for bone turnover. *Int. J. Res. Med. Sci.* **2016**, *4*, 3670–3674. [CrossRef]

14. Abu-Amer, Y. NF-κB signaling and bone resorption. *Osteop. Int.* **2013**, *24*, 2377–2386. [CrossRef] [PubMed]

15. Kalaitzidis, D.; Gilmore, T.D. Transcription factor cross-talk: The estrogen receptor and NF-kappaB. *Trends Endocrinol. Metab.* **2005**, *16*, 46–52. [CrossRef] [PubMed]

16. Ferreira, A.M.; Gentile, P.; Chiono, V.; Ciardelli, G. Collagen for bone tissue regeneration. *Acta Biomater.* **2012**, *8*, 3191–3200. [CrossRef] [PubMed]

17. Nair, A.K.; Gautieri, A.; Chang, S.W.; Buehler, M.J. Molecular mechanics of mineralized collagen fibrils in bone. *Nat. Commun.* **2013**, *1724*. [CrossRef] [PubMed]

18. Poon, B.; Kha, T.; Tran, S.; Dass, C.R. Bone morphogenetic protein-2 and bone therapy: Successes and pitfalls. *J. Pharm. Pharmacol.* **2016**, *68*, 139–147. [CrossRef] [PubMed]

19. Paiva, K.B.S.; Granjeiro, J.M. Bone tissue remodeling and development: Focus on matrix metalloproteinase functions. *Arch. Biochem. Biophys.* **2014**, *1*, 74–87. [CrossRef] [PubMed]

20. Liang, H.P.H.; Xu, J.; Xue, M.; Jackson, C.J. Matrix metalloproteinases in bone development and pathology: Current knowledge and potential clinical utility. *Metall. Med.* **2016**, *3*, 93–102. [CrossRef]

21. Paiva, K.B.S.; Granjeiro, J.M. Matrix Metalloproteinases in Bone Resorption, Remodeling, and Repair. *Prog. Mol. Biol. Transl. Sci.* **2017**, *148*, 203–303. [CrossRef] [PubMed]

22. Lee, Y.M.; Fujikado, N.; Manaka, H.; Yasuda, H.; Iwakura, Y. IL-1 plays an important role in the bone metabolism under physiological conditions. *Int. Immunol.* **2010**, *22*, 805–816. [CrossRef] [PubMed]

23. Zhang, Q.; Chen, B.; Yan, F.; Guo, J.; Zhu, X.; Ma, S.; Yang, W. Interleukin-10 inhibits bone resorption: A potential therapeutic strategy in periodontitis and other bone loss diseases. *BioMed Res. Int.* **2014**, *284836*. [CrossRef] [PubMed]

24. Zarins, J.; Pilmane, M.; Sidhoma, E.; Salma, I.; Locs, J. Immunohistochemical evaluation after Sr-enriched biphasic ceramic implantation in rabbits femoral neck: Comparison of seven different bone conditions. *J. Mater. Sci. Mater. Med.* **2018**, *29*, 119. [CrossRef] [PubMed]

25. Zarins, J.; Pilmane, M.; Sidhoma, E.; Salma, I.; Locs, J. Local and Systemic Morphofunctional Response of Osteoporotic Rabbits Bone Defect Following Implantation of Strontium Doped Biphasic Ceramic Granules. *Solid State Phenomena* **2017**, *267*, 124–131. [CrossRef]

26. Baofeng, L.; Zhi, Y.; Bei, C.; Guolin, M.; Qingshui, Y.; Jian, L. Characterization of a rabbit osteoporosis model induced by ovariectomy and glucocorticoid. *Acta Orthop.* **2010**, *81*, 396–401. [CrossRef] [PubMed]

27. Li, Y.; Chen, S.K.; Li, L.; Qin, L.; Wang, X.L.; Lai, Y.X. Bone defect animal models for testing efficacy of bone substitute biomaterials. *J. Orthopedic Transl.* **2015**, *3*, 95–104. [CrossRef] [PubMed]

28. Calciolari, E.; Donos, N.; Mardas, N. Osteoporotic animal models of bone healing: Advantages and pitfalls. *J. Investig. Surg.* **2017**, *30*, 342–350. [CrossRef] [PubMed]

29. Wancket, L.M. Animal Models for Evaluation of Bone Implants and Devices: Comparative Bone Structure and Common Model Uses. *Vet. Pathol.* **2015**, *52*, 842–850. [CrossRef] [PubMed]

30. Neyt, J.; Buckwalter, J.A.; Carroll, N. Use of animal models in musculoskeletal research. *Iowa Orthop. J.* **1998**, *18*, 118e23.

31. Gilsanz, V.; Roe, T.F.; Gibbens, D.T.; Schulz, E.E.; Carlson, M.E.; Gonzalez, O.; Boechat, M.I. Effect of sex steroids on peak bone density of growing rabbits. *Am. J. Physiol.* **1988**, *255*, E416–E421. [CrossRef] [PubMed]

32. Wang, X.; Mabrey, J.D.; Agrawal, C.M. An interspecies comparison of bone fracture properties. *Bio-Med Mater. Eng.* **1998**, *8*, 1–9.

33. McGovern, J.A.; Griffin, M.; Hutmacher, D.W. Animal models for bone tissue engineering and modelling disease. *Dis. Models Mech.* **2018**, *11*, dmm033084. [CrossRef] [PubMed]

34. Young, S.; Bashoura, A.G.; Borden, T.; Baggett, L.S.; Jansen, J.A.; Wong, M.; Mikos, A.G. Development and characterization of a rabbit alveolar bone nonhealing defect model. *J. Biomed. Mater. Res. A* **2008**, *86*, 182e94. [CrossRef] [PubMed]

35. Dagang, G.; Kewei, X.; Yong, H. The influence of Sr doses on the in vitro biocompatibility and in vivo degradability of single-phase Sr-incorporated HAP cement. *J. Biomed. Mater. Res. A* **2008**, *86*, 947–958. [CrossRef] [PubMed]

36. Gu, Z.; Zhang, X.; Li, L.; Wang, Q.; Yu, X.; Feng, T. Acceleration of segmental bone regeneration in a rabbit model by strontium-doped calcium polyphosphate scaffold through stimulating VEGF and bFGF secretion from osteoblasts. *Mater. Sci. Eng. C Mater. Biol. Appl.* **2013**, *33*, 274–281. [CrossRef] [PubMed]

37. Mohan, B.G.; Shenoy, S.J.; Babu, S.S.; Varma, H.K.; John, A. Strontium calcium phosphate for the repair of leporine (*Oryctolagus cuniculus*) ulna segmental defect. *J. Biomed. Mater. Res. A* **2013**, *101*, 261–271. [CrossRef] [PubMed]

38. Tian, M.; Chen, F.; Song, W.; Song, Y.; Chen, Y.; Wan, C.; Yu, X.; Zhang, X. In vivo study of porous strontium-doped calcium polyphosphate scaffolds for bone substitute applications. *J. Mater. Sci. Mater. Med.* **2009**, *20*, 1505–1512. [CrossRef] [PubMed]

39. Kang, P.; Xie, X.; Tan, Z.; Yang, J.; Shen, B.; Zhou, Z.; Pei, F. Repairing defect and preventing collapse of femoral head in a steroid-induced osteonecrotic of femoral head animal model using strontium-doped calcium polyphosphate combined BM-MNCs. *J. Mater. Sci. Mater. Med.* **2015**, *26*, 80. [CrossRef] [PubMed]

40. Tarafder, S.; Davies, N.M.; Bandyopadhyay, A.; Bose, S. 3D printed tricalcium phosphate bone tissue engineering scaffolds: Effect of SrO and MgO doping on in vivo osteogenesis in a rat distal femoral defect model. *Biomater. Sci.* **2013**, *1*, 1250–1259. [CrossRef] [PubMed]

41. Xie, H.; Wang, Q.; Ye, Q.; Wan, C.; Li, L. Application of K/Sr co-doped calcium polyphosphate bioceramic as scaffolds for bone substitutes. *J. Mater. Sci. Mater. Med.* **2012**, *23*, 1033–1044. [CrossRef] [PubMed]

42. Zhang, Y.; Wei, L.; Chang, J.; Miron, R.J.; Shi, B.; Yi, S.; Wu, C. Strontium-incorporated mesoporous bioactive glass scaffolds stimulating in vitro proliferation and differentiation of bone marrow stromal cells and in vivo regeneration of osteoporotic bone defects. *J. Mater. Chem. B Mater. Biol. Med.* **2013**, *1*, 5711–5722. [CrossRef]

43. Winkler, T.; Sass, F.A.; Duda, G.N.; Schmidt-Bleek, K. A review of biomaterials in bone defect healing, remaining shortcomings and future opportunities for bone tissue engineering: The unsolved challenge. *Bone Joint Res.* **2018**, *7*, 232–243. [CrossRef] [PubMed]

44. Yu, X.; Tang, X.; Gohil, S.V.; Laurencin, C.T. Biomaterials for Bone Regenerative Engineering. *Adv. Healthcare Mater.* **2015**, *4*, 1268–1285. [CrossRef] [PubMed]

45. Cardemil, C.; Elgali, I.; Xia, W.; Emanuelsson, L.; Norlindh, B.; Omar, O.; Thomsen, P. Strontium-doped calcium phosphate and hydroxyapatite granules promote different inflammatory and bone remodelling responses in normal and ovariectomised rats. *PLoS ONE* **2013**, *8*, e84932. [CrossRef] [PubMed]

46. Dondossola, E.; Holzapfel, B.M.; Alexander, S.; Filippini, S.; Hutmacher, D.W.; Friedl, P. Examination of the foreign body response to biomaterials by nonlinear intravital microscopy. *Nat. Biomed. Eng.* **2016**, *1*, 0007. [CrossRef] [PubMed]

47. Anderson, J.M.; Rodriguez, A.; Chang, D.T. Foreign body reaction to biomaterials. *Semin. Immunol.* **2007**, *20*, 86–100. [CrossRef] [PubMed]

48. Barbeck, M.; Dard, M.; Kokkinopoulou, M.; Markl, J.; Booms, P.; Sader, R.A.; Kirkpatrick, C.J.; Ghanaati, S. Small-sized granules of biphasic bone substitutes support fast implant bed vascularization. *Biomatter* **2015**, *5*, e1056943. [CrossRef] [PubMed]

49. Tachibana, Y.; Ninomiya, S.; Kim, Y.; Sekikawa, M. Tissue response to porous hydroxyapatite ceramic in the human femoral head. *J. Orthop. Sci.* **2003**, *8*, 549–553. [CrossRef] [PubMed]

50. Baier, M.; Staudt, P.; Klein, R.; Sommer, U.; Wenz, R.; Grafe, I.; Meeder, P.J.; Nawroth, P.P.; Kasper, C. Strontium enhances osseointegration of calcium phosphate cement: A histomorphometric pilot study in ovariectomized rats. *J. Orthop. Surg. Res.* **2013**, *8*, 16. [CrossRef] [PubMed]

51. Prakasam, M.; Locs, J.; Salma-Ancane, K.; Loca, D.; Largeteau, A.; Berzina-Cimdina, L. Biodegradable Materials and Metallic Implants-A Review. *J. Funct. Biomater.* **2017**, *8*, 44. [CrossRef] [PubMed]

52. Jebahi, S.; Oudadesse, H.; El Feki, H.; Rebai, T.; Keskes, H.; Pellen-Mussi, P.; El Feki, A. Antioxidative/oxidative effects of strontium-doped bioactive glass as bone graft. In vivo assays in ovariectomised rats. *J. Appl. Biomed.* **2012**, *10*, 195–209. [CrossRef]

53. Thormann, U.; Ray, S.; Sommer, U.; Elkhassawna, T.; Rehling, T.; Hundgeburth, M.; Henß, A.; Rohnke, M.; Janek, J.; Lips, K.S.; et al. Bone formation induced by strontium modified calcium phosphate cement in critical-size metaphyseal fracture defects in ovariectomized rats. *Biomaterials* **2013**, *34*, 8589–8598. [CrossRef] [PubMed]

54. Tarafder, S.; Dernell, W.S.; Bandyopadhyay, A.; Bose, S. SrO- and MgO-doped microwave sintered 3D printed tricalcium phosphate scaffolds: Mechanical properties and in vivo osteogenesis in a rabbit model. *J. Biomed. Mater. Res. B Appl. Biomater.* **2015**, *103*, 679–690. [CrossRef] [PubMed]

55. Stipniece, L.; Salma-Ancane, K.; Loca, D.; Pastare, S. Synthesis of strontium substituted hydroxyapatite through different precipitation routes. *Key Eng. Mater.* **2016**, *674*, 3–8. [CrossRef]

56. Grybauskas, S.; Locs, J.; Salma, I.; Salms, G.; Berzina-Cimdina, L. Volumetric analysis of implanted biphasic calcium phosphate/collagen composite by three-dimensional cone beam computed tomography head model superimposition. *J. Cranio Maxill. Surg.* **2015**, *43*, 167–174. [CrossRef] [PubMed]

57. Kiernan, J.A. *Histological and Histochemical Methods: Theory and Practice*; Scion: Bloxham, UK, 2008.

58. Hsu, S.M.; Raine, L.; Fanger, H. Use of avidin–biotin–peroxidase complex (ABC) in immunoperoxidase techniques: A comparison between ABC and unlabeled antibody (PAS) procedures. *J. Histochem. Cytochem.* **1981**, *29*, 577–580. [CrossRef] [PubMed]

59. Pilmane, M.; Rumba, I.; Sundler, F.; Luts, A. Patterns of distribution and occurrence of neuroendocrine elements in lungs of humans with chronic lung disease. *Proc. Latvian Acad. Sci. Sect.* **1998**, *52*, 144–152.